Int. J. Electrochem. Sci., 11 **(2016)** 475 - 485

International Journal of
ELECTROCHEMICAL
SCIENCE
www.electrochemsci.org

Development of the Electrochemical Impedance Response of Ideally Polarized Interfaces Based on Transport Phenomena Laws Through the Nernst-Planck-Poisson Equation Linearized by the Debye-Falkenhagen Approximation.

F. Gómez-Zamudio[1], *R. Antaño-López*[2], *A. Rodríguez-López*[3], *T. Perez*[4], *E. R. Larios-Durán*[1,*]

[1]Universidad de Guadalajara, Departamento de Ingeniería Química, Blvd. Marcelino García Barragán #1451, C.P. 44430, Guadalajara Jalisco, México
[2] Centro de Investigación y Desarrollo Tecnológico en Electoquímica S.C., Pedro Escobedo, C.P. 76703, Querétaro, México
[3] Universidad Politécnica de Santa Rosa Jáuregui. Carretera Federal 57 Qro-SLP km 31-150. Parque Industrial Querétaro, Santa Rosa Jáuregui, Querétaro, Querétaro. C. P. 76220, México
[4]Universidad de Guanajuato, División de Ingenierias, Departamento de Geomática e Hidraulica, Av. Juarez 77, C.P 36000, Guanajuato, Mexico.
[*]E-mail: eroxanita@gmail.com; roxana.larios@red.cucei.udg.mx

Received: 13 October 2015 / *Accepted:* 5 November 2015 / *Published:* 1 December 2015

Physicochemical description of the electrochemical impedance for an ideally polarized interface through the application of Nernst-Planck-Poisson (NPP) model, linearized by Debye-Falkenhagen (D-F) approximation is presented. This description involves physicochemical parameters instead of equivalent circuits. Its simple analytical solution is shown in order to calculate the impedance transfer function, which describes the capacitive contribution to the overall impedance. Model predictions were in qualitative good agreement with the experimental results for Au electrode immersed in 0.1 M and 0.01M KCl. Constant Phase Element (CPE) concept was included in order to provide a closer description to the experimental spectra for solid electrodes in a wide frequency range. Despite these concepts had been deeply explored separately, a connection between them have not been made as in this work.

Keywords: ideally polarized interface, impedance, Nernst-Planck-Poisson model, gold electrode.

1. INTRODUCTION

When an electrode is immersed in an electrolyte, the first phenomenon that takes place at the interface is the formation of the electrochemical double-layer. This is accompanied by a spatial

separation of charge. The comprehension of the structure and properties of charged interfaces started in 1879 with the well-known work developed by Helmholtz and the subsequent improved theories proposed by Gouy, Chapman and Stern. After that, the research focused on the electrochemical double-layer increased throughout the past century until today [1].

As a consequence, this knowledge has been successfully applied in many interest areas such as physical chemistry, engineering, biomedical and in industrial processes [2]. Some properties of the electrochemical double-layer could be experimentally studied by using several techniques such as cyclic voltammetry, chronoamperometry and ac-voltammetry. However, nowadays electrochemical impedance spectroscopy (EIS) is often the most used and reliable technique [3]. According to the conventional interpretation of impedance spectra by using an equivalent circuit approach and based on the double-layer theories, the impedance Z(ω) of an ideally polarized interface is represented by two electrical elements: A capacitor (C_{dl}) coupled in series with the solution resistance (R_s) [4]. The graphical representation of this equivalent circuit in a complex plane depicts a vertical line, which intersects the real axis at a R_s value when high frequencies are reached. Bode-phase diagrams begin near 0º and reach 90º.

When a nearly ideal capacitance is experimentally observed, such as in the cases of mercury drop electrode or presumably single-crystalline electrodes immersed in high-concentrated solutions, a non-linear fitting allows to obtain the electrolyte conductivity as well as the value of the interfacial double-layer capacitance. In several cases, even when an ideally polarized interface is studied, some deviations from an ideal capacitance response could be observed, therefore the impedance spectra in complex representation changes from a vertical to an inclined line and Bode-phase diagrams reaches phase angle values lower than 90º. This behavior can be described by the Constant Phase Element (CPE), which predicts, by a fractional exponent, the dispersive and the frequency-dependent behavior of the double-layer capacitance [5,6]. Following Zoltowski [2], the mathematical expression for impedance of a CPE can be expressed as:

$$Z_{CPE} = \frac{1}{Q_a (j\omega)^n} \quad (1)$$

Where Q_a is a constant in $\Omega^{-1} m^2 s^n$. Similar equations have been published by Lasia [7] and Brug et al. [4]. Despite other mathematical expressions have been given [3], expression (1) is actually accepted and recommended by IUPAC [12]. Usually when frequency dispersion of the capacitance is an experimentally observed effect, a CPE is often included into an equivalent circuit, with a limit $n = 1$ for ideal capacitor and $n = 0$ for a resistor. Then, several investigations based on the CPE concept have been reported in the literature [8-9].

In general, it was proposed that CPE could be originated from surface inhomogeneity [10-11], by the adsorbate diffusion [12], or the electrodes roughness surface [13].

In this way, the interest in the interpretation of CPE parameter *n*, has been increased. Several articles have tried to explain this parameter by fractal dimension [14], electrode roughness effect [11], included vigorous discussions [4-5, 15-17], and the determination of effective capacitance value from CPE element [18].

Beyond the ideality of the interface, the interpretation of EIS spectra by using electrical parameters, either an ideal capacitance or a CPE, is similar because just electric information is reached

when equivalent circuit approach is used, consequently physicochemical information, i.e., adsorbate concentration, diffusion coefficient or Debye length, cannot be directly obtained. Because of that, this work supports the hypothesis that a mathematical impedance model could be obtained from transport phenomena laws, for instance, Nernst-Planck-Poisson (NPP) equations

Solution of NPP equations has been used under different approaches. For instance, the well-known solution of Poisson-Boltzmann equation is often used to calculate the potential profile in the diffuse layer according to the Gouy-Chapman theory [19]. Other more complex applications of the complete NPP model are: the description of the ionic charge densities relaxations [20-22], the description of diffuse layer relaxation at ideally polarized electrodes [23], the prediction of charge density, electric field or electric potential of electrical double-layer [24-27], nanofluidics [28,29] and immittance studies [30-35]. This last approach has been deeply explored by Macdonald and coworkers in a series of publications. Their theoretical developments are very relevant since they were the first ones who analyzed NPP model under several boundary conditions. They subsequently developed the LEVMW software to fit the theoretical immittance expression by complex no linear least-squares with the experimental results. Under this approach, they developed a well-established linear theory of space-charge polarization effects in photoconductors and semiconductors [30]. In a second work [31], they extended their theory, which allowed them to take into account the inclusion of generation and recombination of mobile charges in solids or liquids materials. In [31] the authors use the NPP model to reach a theoretical description of anomalous diffusion for finite-length situations. In addition, Macdonald [32] presented an excellent and complete summary about the history, evolution and the use of NPP and its application to the immitance description of experimental systems. Unfortunately, as Macdonald said in [32]; other authors have not often used the NPP model in order to acquire fundamental descriptions of impedance measurements.

The aim of this paper is to present a physicochemical description of the electrochemical impedance for an ideally polarized interface based on the transport phenomena of the Nernst-Planck-Poisson equation (NPP) linearized by Debye-Falkenhagen (D-F) approximation for a plane geometry. The novelty of our approach is based on simple and novel set of boundary conditions, not previously used, that allow reaching a simple mathematical model as well as its clear and simple analytical solution.

It is worth to note that the main differences between this work and those developed previously by Macdonald are the simple boundary conditions that applies just for a simple electrochemical system instead of generalized conditions proposed for photo and semiconductors given in previous works [30-32]. As a consequence, the model adopted in this work and its notation is considerably simplified. Moreover, its analytical solution is easily reached by using basic mathematical concept such as Laplace as is clearly pointed out. Furthermore, the approach used in this work gives a not complicated formula for the impedance of the system. The simple methodology used in this paper could be an incentive to promote the use of NPP model to other authors interested in the description of impedance spectra from the physicochemical point of view.

In addition, empirical CPE concept was taken into account in order to provide a closer description of experimental data for solid electrodes in a wide frequency range and a new

interpretation of Q_a from equation (1) is proposed. Despite these concepts had been deeply explored separately, a connection between them have not been previously made as in this work.

Finally, we present an experimental example concerning the electrochemical impedance for a gold electrode immersed in 0.1 and 0.01 M KCl interface in absence of faradaic reactions. The experimental measurements were in good agreement with the theoretical prediction given by our model.

2. EXPERIMENTAL PART

For the experimental measurements a conventional three-electrode cell was used. The working electrode was a gold disc electrode (diameter 1.6 mm) embedded in Teflon. The auxiliary electrode was a long Pt wire and the reference was a saturated calomel electrode. The working solutions were 0.1 and 0.01M KCl in water.

Impedance spectra were measured with an Autolab PGSTAT 128N potentiostat controlled by the commercial Nova 1.10 software. The amplitude of perturbation was 10 mV with a frequency range between 10 kHz and 1 mHz. Seven points per logarithm decade were taken. All measurements were carried out at 0.3 V D.C., potential at which no faradaic reaction takes place at the electrode.

Before impedance measurements, a cyclic voltammetry at 50 mV s^{-1} of gold electrode immersed in 0.5 M $HClO_4$ was carried out in order to ensure the cleanliness of the gold electrode interface as well as its reproducibility.

3. MATHEMATICAL MODEL

The mathematical framework starts from the NPP model linearized by Debye-Falkenhagen approximation [36], which can be written as follow [23]:

$$\frac{\partial \rho}{\partial t} = D\frac{\partial^2 \rho}{\partial x^2} - D\kappa^2\rho \quad (2)$$

$$-\varepsilon\frac{\partial^2 \varphi}{\partial x^2} = \rho \quad (3)$$

$$i = -D\frac{\partial \rho}{\partial x} - D\kappa^2\varepsilon\frac{\partial \varphi}{\partial x} \quad (4)$$

Where ρ is the volumetric charge density, ε is the electric permitivity, φ is the electric potential, D is the diffusion coefficient, i is the current density, x is the coordinate away from the electrode and κ is the reciprocal of the Debye thickness given by the following equation:

$$\kappa = \left(\frac{2C^0 z^2 F^2}{\varepsilon RT}\right)^{1/2} \quad (5)$$

in which C^o, z, F,R and T are bulk salt concentration, ion charge, Faraday constant, ideal gas constant and temperature, respectively.

In order to describe an ideally polarized interface, equations (2)-(4) can be solved under the following conditions:

$$\rho(x,0) = 0 \quad (6)$$

$$\rho(\infty,t) = 0 \quad (7)$$

$$\rho(0,t) = -\varepsilon\kappa^2\varphi^0 \quad (8)$$

$$i(0,t) = 0 \quad (9)$$

Condition (6) is related to the electroneutrality, (7) is associated to the charge at semi-infinite distance from the working electrode, (8) is related to the interface condition from Gouy-Chapman theory at low perturbation constraint, where φ^0 is the potential at the electrode surface which is considered time dependent. Finally, (9) is the well-know blocked electrode condition.

Applying Laplace transform to equation (2) and reorganizing, next expression is obtained:

$$s\tilde{\rho} = D\frac{d^2\tilde{\rho}}{dx^2} - D\kappa^2\tilde{\rho} \quad (10)$$

Factorizing $\tilde{\rho}$

$$D\frac{d^2\tilde{\rho}}{dx^2} - (s + D\kappa^2)\tilde{\rho} = 0 \quad (11)$$

Dividing by D, we get the following equation:

$$\frac{d^2\tilde{\rho}}{dx^2} - \left(\frac{s}{D} + \kappa^2\right)\tilde{\rho} = 0 \quad (12)$$

Which has the following solution:

$$\tilde{\rho}(x,s) = C_1e^{-\lambda x} + C_2e^{\lambda x} \quad (13)$$

where

$$\lambda = \sqrt{\frac{s}{D} + \kappa^2} \quad (14)$$

Then, applying the boundary conditions (7) and (8) to equation (13) provides:

$$\tilde{\rho}(x,s) = -\varepsilon\kappa^2\widetilde{\varphi^0}e^{-\lambda x} \quad (15)$$

On the other hand, calculating the Laplace transform of equation (3) and once transformed, substituting it in equation (15) gives:

$$\frac{d^2\tilde{\varphi}}{dx^2} = \kappa^2\widetilde{\varphi^0}e^{-\lambda x} \quad (16)$$

If this equation is integrated once we obtain:

$$\frac{d\tilde{\varphi}}{dx} = -\frac{\kappa^2\widetilde{\varphi^0}e^{-\lambda x}}{\lambda} + B \quad (17)$$

in order to calculate the integration constant B from equation (17), we have transformed the equation (4) and we have evaluated it at the blocked electrode condition (9), in this way the following expression is obtained:

$$\left.\frac{d\tilde{\rho}(x,s)}{dx}\right|_{x=0} = -\kappa^2\varepsilon\left.\frac{d\tilde{\varphi}(x,s)}{dx}\right|_{x=0} \quad (18)$$

which implies

$$\left.\frac{d\tilde{\varphi}(x,s)}{dx}\right|_{x=0} = -\lambda\widetilde{\varphi^0} \quad (19)$$

The substitution of equation (19) on equation (17) generates:

$$\frac{d\tilde{\varphi}}{dx} = -\frac{\kappa^2\widetilde{\varphi^0}e^{-\lambda x}}{\lambda} + \widetilde{\varphi^0}\left(\frac{\kappa^2-\lambda^2}{\lambda}\right) \quad (20)$$

Finally, substituting the derivatives of equation (15) and equation (20) on transformed equation (4) we must reach:

$$\frac{\tilde{\imath}}{\tilde{\varphi}^0} = D\kappa^2\varepsilon\left(\frac{\kappa^2-\lambda^2}{\lambda}\right)(e^{-\lambda x}-1) \quad (21)$$

Which is in fact, the admittance transfer function of an interface when charge transfer is absent, i.e. an ideally polarized interface.

We can evaluate equation (21) at some distance of interest, for instance x= x_h, which correspond to the distance from the working electrode to the Helmholtz plane.

Further simplifications of equation (21), substitution of Laplace variable s by jω and calculating the inverse of admittance, conduce to the impedance transfer function:

$$Z - NPP(\omega) = -\frac{1}{\frac{j\omega\kappa^2\varepsilon A}{\left(\sqrt{\frac{j\omega}{D}+\kappa^2}\right)}\left(e^{-\left(\sqrt{\frac{j\omega}{D}+\kappa^2}\right)x_h}-1\right)} \quad (22)$$

Where A is the area of the working electrode, *j* is the imaginary number and ω is the frequency in rad s^{-1}. Equation (22) predicts the capacitive impedance of an interface as a function of intrinsic parameters such as temperature, concentration, Debye length and diffusion coefficient.

For the sake of completeness, the total impedance of the interface $Z_T(\omega)$ was calculated by adding the contribution of the series resistance Rs.

$$Z_T(\omega) = R_s - \frac{1}{\frac{j\omega\kappa^2\varepsilon A}{\sqrt{\frac{j\omega}{D}+\kappa^2}}\left(e^{-\left(\sqrt{\frac{j\omega}{D}+\kappa^2}\right)x_h}-1\right)} \quad (23)$$

Further simplification of equation (23) can be made if $\left(\sqrt{\frac{j\omega}{D}+\kappa^2}\right)x_h$ is much less than one:

$$Z_T(\omega) = R_s + \frac{1}{j\omega\kappa^2\varepsilon A x_h} \quad (24)$$

This clearly describes the total impedance as an ideal capacitor as a conventional theory but including physicochemical parameters.

In order to predict the deviations from the ideal capacitance behavior, equation (24) was modified by including a fractional exponent *n* on $j\omega$, as is normally done under the CPE approach [2,4,7,12] where it is well known that:

$$C = {Q_a}^{1/n} R_S^{\frac{1-n}{n}} \quad (25)$$

Where C is the effective double-layer capacitance. If we admit from equation (24) that:

$$C = \varepsilon A\kappa^2 x_h \quad (26)$$

The following analogy can be made:

$$\varepsilon A\kappa^2 x_h = {Q_a}^{1/n} R_S^{\frac{1-n}{n}} \quad (27)$$

Thus we can find an interpretation of Q_a in terms of physical parameter, as follow:

$$Q_a = \frac{1}{R_S}(\varepsilon A\kappa^2 x_h R_S)^n \quad (28)$$

And because of equation (28), total impedance can be calculated as follows:

$$Z_T^*(\omega) = R_s + \frac{R_s}{(j\omega\kappa^2\varepsilon A x_h R_s)^n} \quad (29)$$

In a more general case, equation (23) can be modified directly to give:

$$Z_T^{**}(\omega) = R_s - \frac{1}{\frac{(j\omega)^n \kappa^2 \varepsilon' A}{\left(\sqrt{\frac{(j\omega)^n}{D'}+\kappa^2}\right)}\left[e^{-\left(\sqrt{\frac{(j\omega)^n}{D'}+\kappa^2}\right)x_h} - 1\right]} \quad (30)$$

Where D' in $m^2\ s^{-n}$ and ε' in $F\ s^{n-1}\ m^{-1}$ are not precisely the common coefficient diffusion and electric permittivity.

4. RESULTS AND DISCUSSION

Several simulations using equation (30) were carried out using Matlab software. The good theoretical prediction of equation (30) is shown in Fig. 1. In all cases we used $D' = 2x10^{-9}\ m^2\ s^{-n}$ [37], z = 1, $\varepsilon' = 6.94x10^{-10}\ F\ s^{n-1}\ m^{-1}$ [19] (aqueos solutions), $x_h=1x10^{-9}$ m [38], $R_s=1000\ \Omega\square\square\square\square\square x10^{-6}\ m^2$. For Figure 1a and 1b *n* was shifted from 0.1 to 0.7, meanwhile for Figure 1c, *n* was fixed *to 0.9* and C^o were changed from 1M to 1mM.

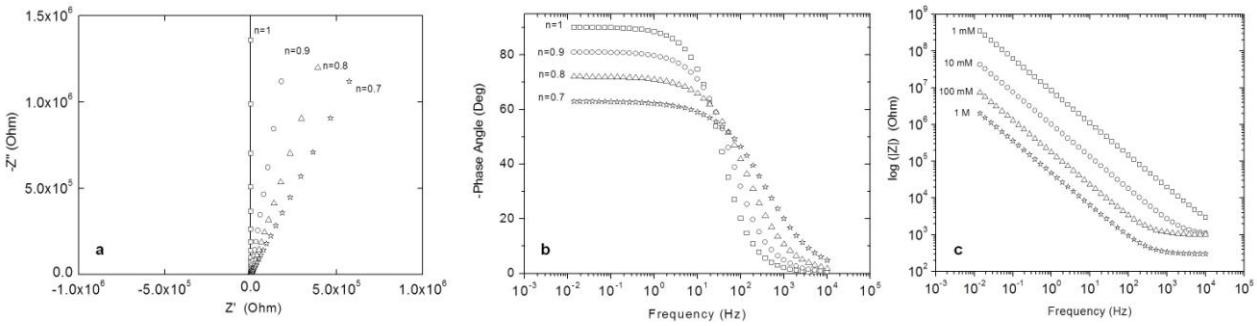

Figure 1. Theoretical a) complex, b) Bode-phase and c) Bode-modulus electrochemical impedance diagrams calculated by equation (30) at different *n* values and different concentrations.

The Fig. 1 a and b depict the effect on the CPE parameter in equation (30). It is possible to recognize the typical response of complex impedance for an ideally polarized interface including both cases: an ideal and non-ideal capacitance. When an ideal capacitance is taking into account, the equation (30) is used with *n*=1. The theoretical prediction is a vertical line in the complex plane (Fig. 1a) and the Bode-phase diagram (Fig. 1b) starts from zero and reaches values of 90º. When frequency dispersion is included, equation (30) is employed with different *n* values, from 0.9 to 0.7. In these cases, diagonal line is depicted in the complex plane of the impedance and as is evidenced from the Bode-phase diagram, the phase angle decreases when *n* value diminishes, in agreement with the equation [3,5]:

$$Z_{CPE} = \frac{1}{\omega^n A_0}\left[cos\left(\frac{n\pi}{2}\right) - jsin\left(\frac{n\pi}{2}\right)\right] \quad (31)$$

On the other hand, the concentration effect on equation (30) is evidenced in Fig. 1c. The response shown in Fig. 1c was obtained for n=0.9, meanwhile C° was modified. Bode-modulus diagram shows that the impedance modulus decreases at the whole frequency range when concentration increases, as is expected. Even more, for the more concentrate solutions, the typical resistive response is clearly defined at the high frequency limit and subsequently, when frequencies decrease the capacitance contribution to the total impedance is observed as a diagonal line with a negative slope.

4.1. Experimental and theoretical data comparison

Fig. 2 shows the Bode-modulus and Bode-phase diagrams obtained for gold/KCl interface at 0.3 V vs. SCE, room temperature and two chloride ion concentration, 0.1 (Fig 2a) and 0.01M (Fig 2b).

For both concentrations, Bode-modulus diagrams depict a diagonal line that describes the predominant capacitive behavior of the interface even at so low frequencies such as 0.01 Hz. On the other hand, Bode-phase diagrams confirm the tendencies described above, and furthermore, clearly evidence the dispersive double-layer capacitance effects, which generate phase angles lower than 90º as is expected for a CPE behavior-like. It is worth to note that the deviations from the ideal capacitance behavior are slightly higher when ions concentration diminishes; this experimental fact is in good agreement with previous reports [12, 23]. We associate the dispersive double-layer capacitance effects to the roughness and polycrystalline nature of the work electrode as well as the chloride adsorption mass transfer, which is also evidenced at low concentration of ions [4, 12,13].

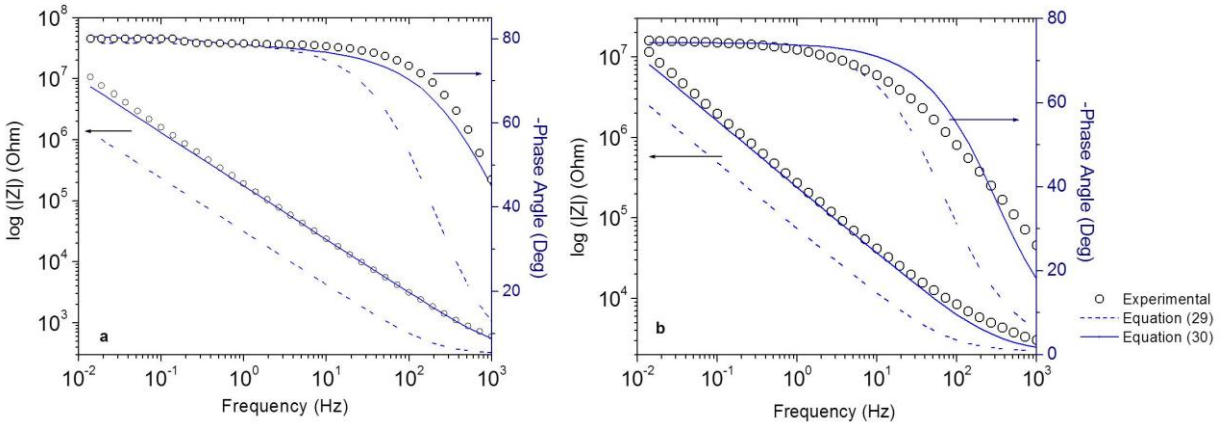

Figure 2. Theoretical prediction of Bode diagrams obtained by equations (29) (dashed line), (30) (continued line) and the comparison with the experimental measurements (open dots) for gold/KCl interface at 0.3 mV at a) 0.1M and b) 0.01M chloride concentration.

Before comparing the experimental measurement with the theoretical prediction of our model, a fitting under equivalent circuit approach using CPE element was carried out through Zview software.

Once the exponential *n* of the CPE element and Rs were obtained, they were used on equations (29) and (30).

Comparison between simulations of equations (29)-(30) as dashed and continuous lines, and the experimental data as open dots are shown in Fig. 2. Table 1 summarizes the parameters used in the theoretical response. From Fig. 2 is noted that when equation (29) is used, the impedance predicted is underestimated at the whole frequencies evaluated. A better approximation is obtained when equation (30) is employed, and its best approximation is reached at highest concentration as is noted in Figure 2a.

Table 1. Physicochemical parameters used in the simulations.

C^o / mol m^{-3}	Rs / Ohms	D / m^2 s^{-1}	κ / m^{-1}	x_h / m	n /
10	2167	$2x10^{-9}$	$3.2x10^{8}$	$1.8x10^{-10}$	0.82
100	280	$2x10^{-9}$	$1x10^{9}$	$1.8x10^{-10}$	0.9

In general, the results obtained by equation (30) are in qualitative good agreement with fundamental aspects of the double layer. For instance, impedance magnitude decreases when salt concentration increases as is observed at the high frequency limit and, on the other hand, the diffusion coefficient is in good agreement with the value previously reported [37]. Furthermore, x_h correspond to the ionic radius of chloride [38].

In contrast to the typical equivalent circuit method, a physicochemical description of the interface is reached under this approach. Moreover, the clear and simple mathematical framework employed to acquire the analytical expression of impedance, should be highlighted. Extension of our model to different electrolyte stoichiometry and different electrode geometries, such as spherical or cylindrical, could be derived. However, its deduction deserves a deeper exploration and will be subject of our future work.

5. CONCLUSIONS

A mathematical model based on Nernst-Planck-Poisson equation linearized by Debye-Falkenhagen approximation was developed to calculate the electrochemical impedance transfer function of an ideally polarized interface with a plane geometry and simple 1:1 electrolyte. The model was analytically solved using Laplace Transform. The model can predict the impedance related to an ideal double-layer capacitance as well as the frequency dispersion of this thermodynamic parameter. Despite these concepts have been deeply explored separately, a connection between them have not been made as in this work.

In this way, electrochemical impedance is described by physical parameters like diffusion coefficient, temperature and ions concentrations.

ACKNOWLEDGEMENTS
The authors acknowledges to CONACYT for financial support through project CB-169379. Felipe Gómez-Zamudio acknowledges the scholarship granted by CONACYT.

References

1. B. B. Damaskin and O. A. Petrii, *J. Solid State Electr.*, 15 (2011) 1317.
2. P. Zoltowski, *J. Electroanal. Chem.*, 443 (1998) 149.
3. J. R. Macdonald, *Impedance Spectroscopy, Emphasizing Solid Materials and Systems*, Willey, New York (1987).
4. G. J. Brug, A. L. Van den Eeden, M. Sluyters-Rehbach and J. H. Sluyters, *J. Electroanal. Chem.*, 176 (1984) 275.
5. J. R Macdonald, *Solid State Ionics*, 13 (1984) 147.
6. M. Orazem and B. Tribollet, *Electrochemical Impedance Spectroscopy*, John Wiley & Sons. Inc., New Jersey (2008).
7. A. Lasia, *Electrochemical Impedance Spectroscopy and its Applications, Springer, New York (2014).*
8. J. Jorcin, M. E. Orazem, N. Pébère and B. Tribollet, *Electrochim. Acta*, 51 (2006) 1473.
9. H. Fricke, *Philos. Mag*, (7) 14, (1932) 310.
10. M. Kramer and. M. Tomkiewicz, *J. Electrochem. Soc.*, 131 (1984) 1283.
11. Z. Kerner and T. Pajkossy, *J. Electroanal. Chem.*, 448 (1998) 139.
12. M. Sluyters-Rehbach, *Pure Appl. Chem.*, 66 (1994) 1831.
13. R. de Levie, *Electrochim. Acta*, 9 (1964) 1231.
14. L. Nyikos and T. Pajkossy, *Electrochim. Acta*, 30 (1985) 1583.
15. G. Láng and K. E. Heusler, *J. Electroanal. Chem.*, 457 (1998) 257.
16. A. Sadkowski, *J. Electroanal. Chem.*, 481 (2000) 222.
17. Z. Kerner and T. Pajkossy, *Electrochim. Acta*, 46 (2000) 207.
18. B. Hirschorn, M. E. Orazem, B. Tribollet, V. Vivier, I. Frateur and M. Musiani, *Electrochim. Acta*, 55 (2010) 6218.
19. A. J. Bard and L. R. Faulkner, *Electrochemical Methods. Fundamentals and Applications*, John Willey & Sons, Inc., New York (2001)
20. M. Pabst, G. Wrobel, S. Ingebrandt, F. Sommerhage and A. Offenhäusser, *Eur. Phys. J. E*., 24 (2007) 1.
21. A. Golovnev and S. Trimper, *J. Chem Phys.*, 131 (2009) 114903.
22. A. Golovnev and S. Trimper, *J. Chem Phys.*, 134 (2011) 154902.
23. R. P. Buck, *Electroanal. Chem.*, 23 (1969) 219.
24. J. Lim, J. Whitcomb, J. Boyd and J. Varghese, *J. Colloid Interf. Sci.*, 305 (2007) 159.
25. M. Z. Bazant, K. Thornton, and A. Ajdari, *Phys. Rev. E.*, 70 (2004), 021506-1.
26. J. Hsa, Y. Kuo and S. Tseng, *J. Colloid Interf. Sci.*, 195 (1997) 388.
27. F. Beunis, F. Strubbe, M. Marescaux, J. Beeckman, K. Neyts, and A. R. M. Verschueren, *Phys. Rev. E.*, 78 (2008) 011502.
28. Y. S. Choi and S. J. Kim, *J. Colloid Interf. Sci.*, 333 (2009) 672.
29. C. Chang and R. Yang, *J. Colloid Interf. Sci.*, 339 (2009) 517.
30. J. Ross Macdonald, *Phys. Rev.*, 92 (1953) 4.
31. J. Ross Macdonald and D. R. Franceschetti, *J. Chem. Phys.*, 68 (1978) 1614.
32. J. Ross Macdonald, L. R. Evangelista, E. K. Lenzi and G. Barbero, *J. Phys. Chem. C.*, 115 (2011) 7648.
33. J. Ross Macdonald, *J. Phys. Chem. C.*, 117 (2013) 23433.
34. E. J. F. Dickinson and R. Compton, *J. Electroanal. Chem.*, 655 (2011) 23.

35. E. K. Lenzi, M. K. Lenzi, F. R. G. B. Silva, G. Goncalves, R. Rossato, R. S. Zola and L. R. Evangelista, *J. Electroanal. Chem.*, 712 (2014) 82.
36. P. Debye and H. Falkenhagen, *Physik. Z.*, 29 (1928) 121.
37. Z. Kerner and T. Pajkossy, *Electrochim. Acta*, 47 (2002) 2055.
38. M. A. V. Devanathan and B. V. K. S. R. A. Tilak, *Chem Rev.*, 65 (1965) 635.